Title
Spatial diversity in passive time reversal communications

Permalink
https://escholarship.org/uc/item/1tb7x730

Journal
Journal of the Acoustical Society of America, 120(4)

ISSN
0001-4966

Authors
Song, Hee C
Hodgkiss, W S
Kuperman, W A
et al.

Publication Date
2006-10-01

Peer reviewed

Spatial diversity in passive time reversal communications

H. C. Song,[a)] W. S. Hodgkiss, W. A. Kuperman, W. J. Higley, K. Raghukumar, and T. Akal
Marine Physical Laboratory, Scripps Institution of Oceanography, La Jolla, California 92093-0238

M. Stevenson
NATO Undersea Research Centre, La Spezia, Italy

A time reversal mirror exploits spatial diversity to achieve spatial and temporal focusing, a useful property for communications in an environment with significant multipath. Taking advantage of spatial diversity involves using a number of receivers distributed in space. This paper presents the impact of spatial diversity in passive time reversal communications between a probe source (PS) and a vertical receive array using at-sea experimental data, while the PS is either fixed or moving at about 4 knots. The performance of two different approaches is compared in terms of output signal-to-noise ratio versus the number of receiver elements: (1) time reversal alone and (2) time reversal combined with adaptive channel equalization. The time-varying channel response due to source motion requires an adaptive channel equalizer such that approach (2) outperforms approach (1) by up to 13 dB as compared to 5 dB for a fixed source case. Experimental results around 3 kHz with a 1 kHz bandwidth illustrate that as few as two or three receivers (i.e., 2 or 4 m array aperture) can provide reasonable performance at ranges of 4.2 and 10 km in 118 m deep water. © *2006 Acoustical Society of America.* [DOI: 10.1121/1.2338286]

I. INTRODUCTION

Recently time reversal has attracted attention in underwater acoustic[1–3] and wireless channel[4–6] communications. Time reversal typically involves a source/receive array referred to as a time reversal mirror (TRM) which samples the incoming field generated by a probe source (PS). When the received signals are played back in a time-reversed fashion, they converge to the PS location without a priori knowledge of the channel.[7,8] In a multipath environment, the time reversal process also undoes the multipath and recovers the original PS signal at the focus. The spatial and temporal focusing (pulse compression) capability of time reversal immediately offers potential application to communications, especially in an environment with significant multipath. The temporal compression mitigates the inter-symbol interference (ISI) resulting from multipath propagation, while the spatial focusing achieves a high signal-to-noise ratio (SNR) at the intended receiver with a low probability of interception elsewhere. The benefit of the time reversal approach is a simple receiver structure (complexity) as opposed to the high computational complexity required for multi-channel adaptive equalizers.[9]

The preliminary system concept for active time reversal communications has been demonstrated experimentally in shallow water using a 29 element, 78 m aperture TRM, operating in the 3–4 kHz band.[1] While the temporal focusing achieved by time reversal reduces ISI significantly, there always is some residual ISI which results in a saturation of the performance at high SNR.[10] In addition, the channel varies over time in a fluctuating environment. Recently it was confirmed using at-sea experimental data[11,12] that the performance of time reversal alone can be improved significantly in conjunction with adaptive channel equalization which simultaneously removes the residual ISI and compensates for the channel variations. Indeed, Song *et al.*[12] have shown that the combination provides nearly optimal performance using the theoretical performance bounds derived in Ref. 10. Furthermore, time reversal communications have been extended to multiple-input/multiple-output multi-user communications exploiting the spatial focusing property and linearity of the system such that independent messages were sent simultaneously from a TRM (base station) to multiple receivers (users) at 8.6 km range in 105 m deep water.[13]

Passive time reversal also has been studied in the literature where the TRM needs only to receive. Reciprocity is invoked to relate passive and active time reversal and the two approaches basically are equivalent while the communication link is in the opposite direction. Indeed, the two approaches provide the same performance in theory under ideal circumstances.[10] Dowling[14] suggested the method would be useful for pulse compression and acoustic communications. Instead of rebroadcasting the wave fronts observed at a TRM, passive time reversal is implemented numerically at the receiver using the measured channel response which requires a channel probe transmission followed by the information-bearing signal[3] (see Fig. 2). Silva *et al.*[2] proposed a virtual TRM implemented electronically at the receiver array and evaluated the performance by numerical simulations. Experimental demonstration of passive time reversal was reported by Rouseff *et al.*[3] using a 14-element array, operating in the 5–20 kHz band, up to 5 km range in water between 10 and 120 m deep. The probe source was either fixed or drifting at less than 1 knot. To account for the

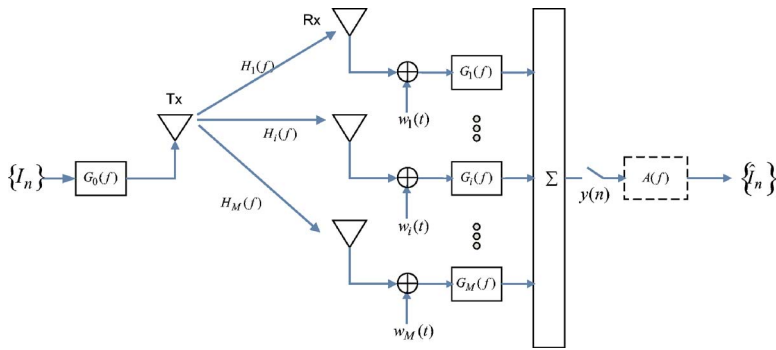[a)]Author to whom correspondence should be addressed; electronic mail: hcsong@mpl.ucsd.edu

FIG. 1. (Color online) System model for passive time reversal communications followed by an equalizer (dashed box).

channel temporal variability, however, the probe signal had to be reinserted frequently to capture updated channel responses, effectively reducing the data rate by a factor of 2. To diminish the loss in data rate, a decision-directed passive phase conjugation (DDPPC) approach has been developed by the same group,[15] in which the current block of data is used to update an estimate of the channel for the next block.

As described above, both active and passive time reversal communications employ a vertical receiver array in a waveguide spanning the water column with many elements to sufficiently sample the incoming field for maximal time reversal focusing. A natural question that follows is how many elements (or how large an array aperture) are required to provide reasonable performance for practical applications of the time reversal approach. The objective of this paper is to study the impact of spatial diversity in passive time reversal communications between a single PS and a vertical receiver array, while the results are equally applicable to the active time reversal case. We take advantage of the passive time reversal approach which allows selecting a subset of array elements from a single transmission for comparison purposes. The PS is either fixed or moving.

To achieve the objective, we investigate the performance of two different approaches using at-sea experimental data in terms of output SNR as a function of the number of receiver elements: (1) time reversal alone and (2) time reversal combined with adaptive channel equalization. In the latter, channel equalization is applied to a single time series which is combined from multi-channel data using the time reversal concept (see Fig. 1), whereas multi-channel equalization typically involves (feedforward) filters applied to each channel that are updated jointly and then followed by channel combining.[9,16,17] Since time reversal is analogous to broadband matched-field processing (or generalized beamforming),[7,18,19] approach (2) can be viewed as a generalized beam former followed by channel equalization. The benefit of this approach is that the number of taps required for the

post-time reversal equalizer is much smaller than the case with just an equalizer alone, thereby resulting in lower computational complexity of the equalizer.[12,20]

This paper will present experimental results of coherent passive time reversal communications between a probe source and a 32 element vertical receiver array with 2 m spacing in 118 m deep water, operating around 3 kHz with a 1 kHz bandwidth during the focused acoustic fields 2004 (FAF-04) experiment. The theory behind passive time reversal communication is briefly reviewed in Sec. II. Section III describes the experimental setup and Sec. IV analyzes the performance for a fixed source at 10 km range. The performance analysis for a moving source at 4.2 km range is presented in Sec. V.

II. PASSIVE TIME REVERSAL: THEORY

The theory behind the use of active time reversal in the context of acoustic communications has been described in our earlier paper[1] where two-way time reversal can be seen as implementing actively a spatio-temporal matched filter of the channel response (Green's function) from a signal processing point of view. On the other hand, one-way passive time reversal requires only a receiver array and the spatio-temporal matched filter is implemented numerically at the receiver. The overall system under consideration is shown in Fig. 1 where passive time reversal is followed by an equalizer when necessary. An extensive discussion on passive time reversal communications also can be found in Ref. 3.

When a known signal $g_0(t) = s(t)$ is transmitted from a PS in a waveguide, the (noiseless) received signal on the ith element of a receiver array is $r_i(t) = s(t) * h_i(t)$ where $h_i(t)$ is the channel impulse response of the waveguide and $*$ denotes convolution. While active time reversal retransmits the time reversed version of the received signal $r_i(-t)$[12], passive time reversal applies matched filtering at each receiver element with $g_i(t) = h_i(-t)$ and combines them coherently such that

$$y(t) = \sum_{i=1}^{M} r_i(t) * g_i(t) = s(t) * \left[\sum_{i=1}^{M} h_i(t) * h_i(-t) \right]$$
$$= s(t) * q(t), \tag{1}$$

where M is the number of receiver elements and the term in the right bracket is denoted the q function representing the summation of the autocorrelation of each channel impulse response.[21] It should be mentioned that $y(t)$ is essentially
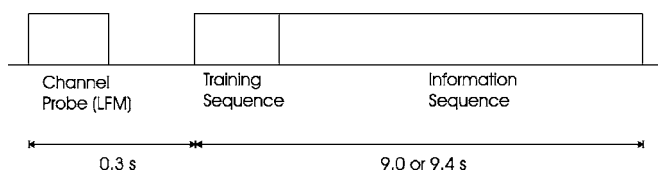

FIG. 2. Typical data format transmitted by a probe source for passive time reversal communications. The overhead resulting from a probe signal transmission and 100 training symbols is less than 5%.

identical to the signal received at the probe source position in active time reversal $s_{ps}(-t)$ [Eq. (1) in Ref. 12]. Note that the matched filter in the frequency domain $G_i(f)=H_i^*(f)$ requires knowledge of the channel which can be obtained by a channel probe signal prior to the information-bearing signals as shown in Fig. 2. The performance of time reversal focusing depends on the complexity of the channel $h_i(t)$ (i.e., the number of multipaths), the number of array elements M, and their spatial distribution.

The application of time reversal to communications, either active or passive, relies totally on the behavior of the q function in Eq. (1). To minimize the ISI, it would be desirable to have a q function that approaches a delta function. In practice, however, there always is some residual ISI which results in a saturation of the performance.[10,22] Moreover, the channel continues to evolve over time in a dynamic ocean environment while time reversal assumes that the channel is time invariant. Thus time reversal alone may require frequent transmission of a channel probe signal at the expense of data rate to account for channel fluctuations[3] while the loss in data rate can be somewhat diminished by the DDPPC approach[15] as mentioned in Sec. I. In this paper, the passive time reversal approach will be combined with adaptive channel equalization to simultaneously eliminate the residual ISI and compensate for channel fluctuations without compromising the data rate. This is especially true for a moving source as will be shown in Sec. V.

III. EXPERIMENT

A time reversal experiment was conducted jointly with the NATO Undersea Research Center in July 2004 both north and south of Elba Island, off the west coast of Italy.[12] The passive time reversal communications experiment reported in this paper was carried out in a flat region of 118 m deep water north of Elba on July 17 (JD199). A 32-element vertical receiver array (VRA) was deployed spanning the water column from 42 to 104 m with 2 m element spacing which corresponds to about 4λ at 3 kHz. Sound speed profiles collected during the experiment are shown in Fig. 3 featuring an extended thermocline down to 70 m depth. The VRA was moored for stable operation. The probe source was either fixed at 90 m depth (+) or moving at 70 m depth (○) as marked in Fig. 3. We begin with analysis of the stationary source data in the next section.

IV. PERFORMANCE: STATIONARY SOURCE

In this section, the performance of passive time reversal communications is addressed between a stationary source and the VRA separated by 10 km as shown in Fig. 4(a). For a fixed probe source, a single element at 90 m depth was selected from a source/receiver array which we have used previously for active time reversal communications.[12] The source level was 179 dB *re* 1 μPa. The probe signal $g_0(t)$ was a 150 ms, 2.5–4.5 kHz linear frequency modulation (LFM) chirp with a Hanning window, resulting in an effective 100 ms, 3–4 kHz bandwidth chirp. Note that this probe signal is identical to the one used for active time reversal communications reported in Refs. 12 and 13 and the duration
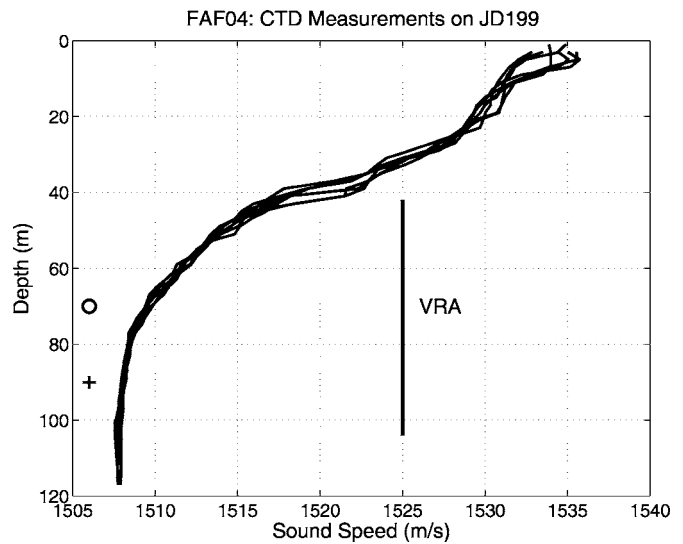

FIG. 3. The sound speed profile measured during the passive time reversal communications experiment on July 17, 2004 (JD199) along with the depth coverage of the VRA. The probe source depths are also denoted: fixed (+) and moving (○).

of the chirp after compression (matched filtering) is $T=2$ ms. Binary phase-shift keying (BPSK) was used to encode the data stream with a symbol rate of $R=1/T=500$ symbols/s such that the 150 ms chirp signal $g_0(t)$ was overlapped every 2 ms with polarity ± 1 to generate the information-bearing signal $v(t)=\Sigma_n I_n g_0(t-nT)$. $\{I_n\}$ is the sequence of information symbols and $g_0(t)$ is applied as a shaping (modulation) filter (see Fig. 1). The communications sequence was 9.4 sec long with $N=4700$ symbols as shown in Fig. 2 and the sampling frequency was $f_s=12$ kHz. The resulting spectral efficiency is 0.5 bit/s/Hz for a 1 kHz bandwidth. It should be pointed out that the overhead resulting from the probe transmission and 100 training symbols reduces the data rate by less than 5%.

The channel response captured by the VRA from the PS at 10 km range is displayed in Fig. 4(b) showing a complicated multipath structure in an acoustic waveguide. The received signal is noisy even after compression of the chirp wave form with SNRs of 1.5–7.8 dB depending on the receiver depth. The delay spread is about 40 ms resulting in an ISI of 20 symbols. The measured channel response (before compression) will be used as a demodulation filter $g_i(t)$ in Fig. 1 such that $g_i(t)=g_0(-t)*h_i(-t)$ for matched filtering of both the probe signal and the channel impulse response at once. Before discussing spatial diversity with multiple receiver elements, the performance of a single receiver is investigated.

A. Single receiver: $M=1$

The performance of single element processing is illustrated in Fig. 5(a) in terms of bit error rate (BER) and output signal-to-noise ratio (SNR_o) at the receiver depth using two different approaches: (1) time reversal alone (Δ) and (2) time reversal combined with adaptive channel equalization (○). The output SNR_o (normalized by the signal energy)[23] is the reciprocal of the mean-square error (MSE) denoted by J,
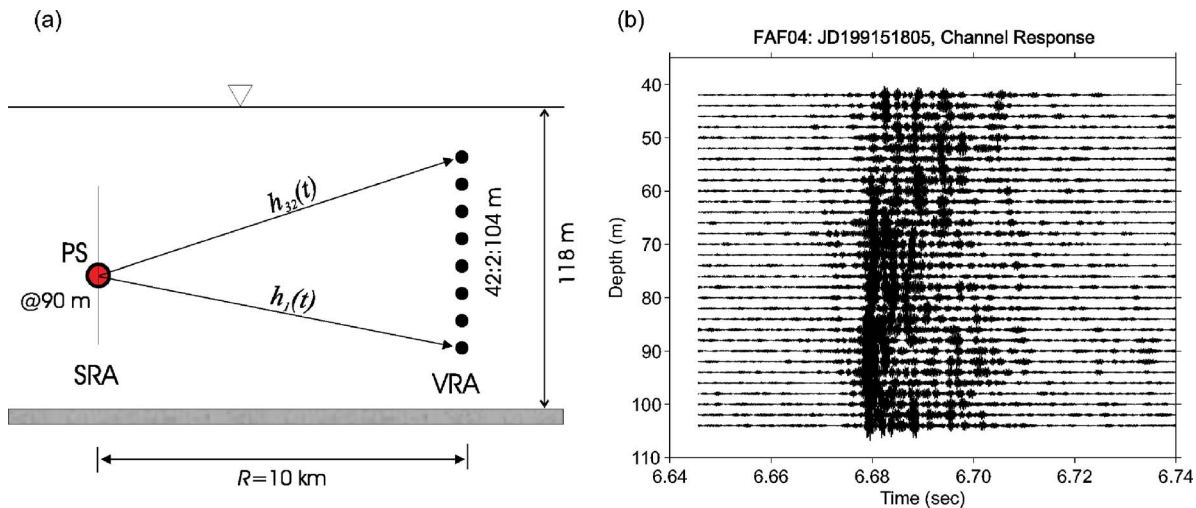
FIG. 4. (Color online) (a) Schematic of passive time reversal communication with a stationary probe source. (b) The channel responses (after compression) received by the VRA from a probe source at 90 m depth and 10 km range.

$$J = \text{SNR}_o^{-1} = E|I_n - \hat{I}_n|^2, \qquad (2)$$

where E denotes expectation, I_n is the information symbol (± 1) and $\hat{I}_n$ is the estimate of that symbol. Examples of scatter plots with $\{\hat{I}_n\}$ are shown in Fig. 5(b) for two different receiver depths: 46 and 78 m. For convenience, the scatter plots displayed throughout this paper are normalized with respect to the maximum value of $\{|\hat{I}_n|\}$. To estimate the input SNR (∗), noise power is calculated outside the communication signal interval (before and/or after) while signal-plus-noise power is calculated within the communication signal interval. The difference between the two calculations is an estimate of the signal power. The input SNR (∗) is superimposed in Fig. 5(a). The receiver for approach (1) is identical to the optimum receiver for signals corrupted by added white Gaussian noise in the absence of ISI[24] while the receiver for approach (2) is described in Ref. 12. Phase tracking was carried out by using

a decision-feedback phase-locked loop (DFPLL)[24] averaged over 20 symbols.

Two observations can be made. First, the combination (○) always outperforms time reversal alone (△) although the improvement is minimal at low input SNR (∗). It is interesting that even a single receiver at 78 m depth provides reasonable performance (BER=0.4%, SNR$_o$=6.5 dB) for an input SNR of 7 dB [see Fig. 5(b)]. The BER is under 20% for all receivers where the input SNR is relatively low at levels of 1.5–7.8 dB. In general, a higher input SNR yields better performance.

An adaptive equalizer, either linear feedforward or nonlinear decision feedback (DFE) whichever yields better performance, has been applied independently to each receiver. Interestingly, it is found that when the BER of time reversal alone exceeds about 10%, a linear equalizer usually outperforms a nonlinear DFE which uses previously detected symbols to suppress the ISI in the present symbol. Since the
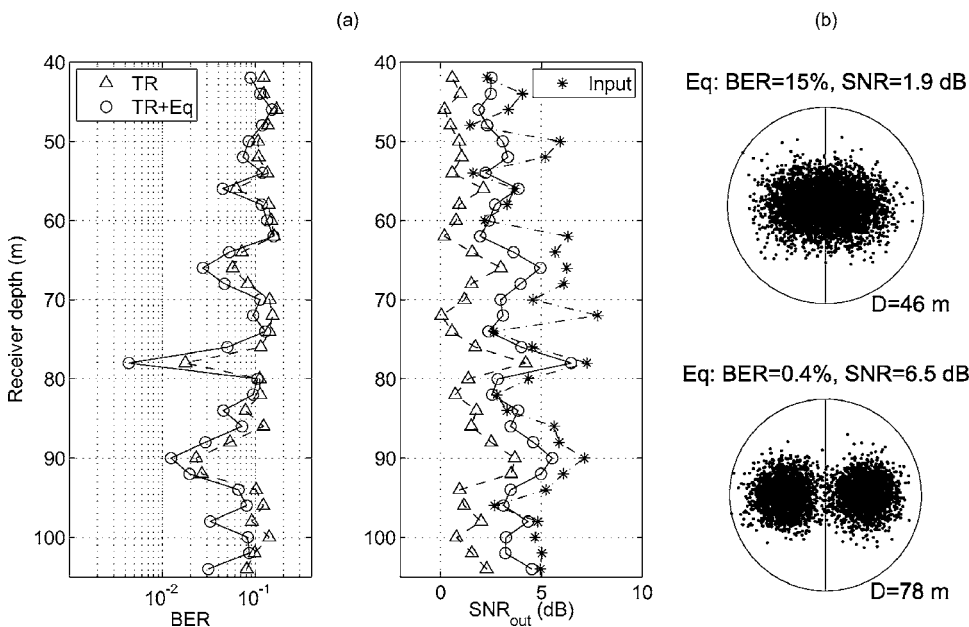

FIG. 5. Performance of single element processing: time reversal alone (△) and time reversal combined with an adaptive channel equalizer (○). (a) BER and output SNR$_o$ as a function of receiver depth. The input SNR (∗) is also displayed on the right column. (b) Example of scatter plots of time reversal combined with channel equalization for two different receiver depths: D=46 m (SNR$_o$=1.9 dB) and D=78 m (SNR$_o$=6.5 dB).
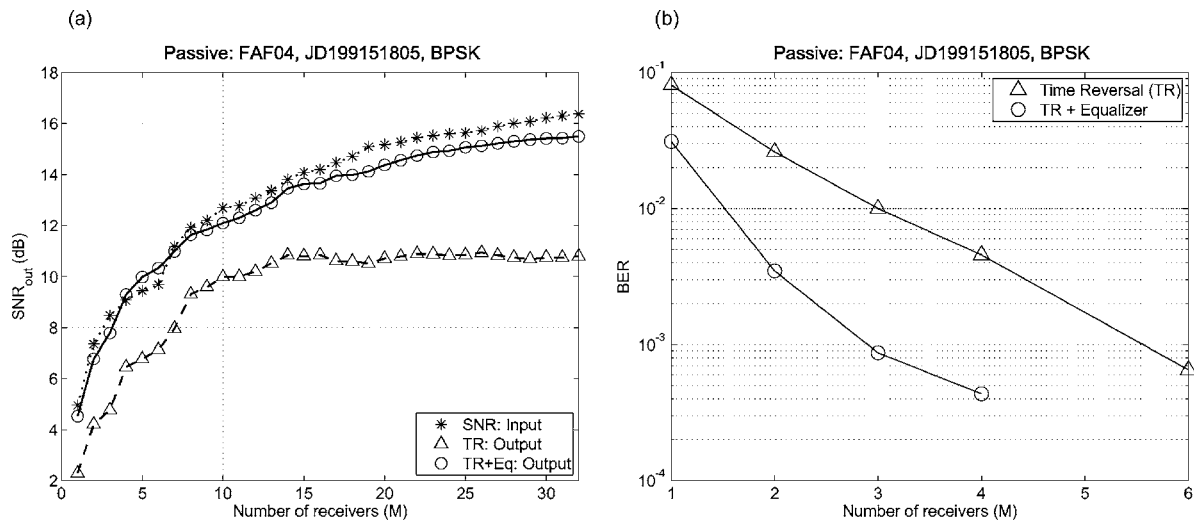
FIG. 6. Performance of multi-channel processing as a function of the number of receiver elements M: time reversal alone (Δ) and time reversal combined with an adaptive DFE equalizer ($\bigcirc$). The receiver elements are selected from the bottom (see Fig. 4). (a) Output SNR_o along with input SNR ($*$). (b)BER. There are no errors beyond the M marked.

symbol rate $R=500$ symbols/s is only half the signal bandwidth of 1 kHz, a fractionally spaced equalizer (FSE) with feedforward tap spacing of $(1/2)T$ or less should be used to avoid compensating for the aliased received signal. Here we use a tap spacing of $(1/4)T$ as in active time reversal communications resulting in the best performance.[12] The number of taps for feedforward filters n_f varies from 8 to 40. Note that even with $n_f=40$ spans only half the 20 symbols of ISI are shown in Fig. 4(b) due to the temporal compression provided by the time reversal process, which is the benefit of the combined approach ($\bigcirc$) as described in Sec. I. The recursive least squares (RLS) algorithm has been used for implementing the adaptive equalizer with forgetting factor 0.995.

It also is interesting to observe that the performance at shallower depths (around 40–60 m) appears worse in general than at deeper depths, which can be explained as follows. First, generally the energy at shallower depths is smaller than at deeper depth due to the sound speed profile shown in Fig. 3 where the energy tends to refract downward. Second, the receivers at shallower depths are located in the middle of thermocline, where they are more susceptible to environmental fluctuations.

B. Multiple receivers

The impact of spatial diversity is illustrated in Fig. 6 where the performance of time reversal communications is shown as a function of the number of receivers M in terms of (a) output SNR_o and (b) BER for two different approaches as before: time reversal alone (Δ) and time reversal combined with an adaptive DFE ($\bigcirc$). The elements are selected sequentially from the bottom such that, for example, $M=4$ includes the bottom-most four elements. Note that the horizontal axis can be replaced by aperture of the corresponding subarray ranging from 0 to 62 m. Here a nonlinear adaptive DFE has been used to generate the results of Fig. 6 which yields better performance. The number of taps used for the feedforward and feedback portions of the DFE are $n_f=20$ and $n_b=4$, respectively, and the RLS forgetting factor is

0.995. In Fig. 6(b), there are no errors beyond the M marked. Recall from Fig. 1 that the equalization is applied to a single time series which is combined from multichannel data. Phase tracking is also carried out on the single time series using a DFPLL prior to the channel equalization.

Note that the performance of time reversal (Δ) improves quite rapidly (almost linear) up to about $M=10$ (i.e., 20 m aperture), then slowly increases and eventually saturates. This happens when there is no additional gain from spatial diversity given the channel complexity and the side lobe levels of q function remain unchanged. On the other hand, the performance of time reversal combined with adaptive channel equalization ($\bigcirc$) continues to improve as the number M increases although the enhancement is gradual as compared to the significant improvement with the first several elements. This observation indicates that spatial diversity can be exploited maximally using a few elements with a small aperture given the environmental complexity. Overall, the combination outperforms time reversal alone from 2 dB up to 5 dB. In addition, the output SNR_o ($\bigcirc$) is almost comparable to the input SNR ($*$).

Taking advantage of spatial diversity requires an appropriate element spacing to ensure that the channel impulse responses are sufficiently different from one another.[22] Thus the side lobes of the autocorrelation function of each channel response interfere destructively, while the main lobes of the autocorrelation functions add up coherently in the q function. The VRA element spacing is 2 m which corresponds to $\sim 4\lambda$ at 3.5 kHz and apparently provides sufficient element spacing across the array in Fig. 4(b). One way to confirm that there is sufficient spacing between the elements is to compare the performance of different sets of receiver elements for a fixed M (e.g., $M=4$) and we did not find any noticeable differences.

A few examples of scatter plots corresponding to Fig. 6 are displayed in Fig. 7 when $M=1$, 2, 4, and 32. The top panels illustrate that the $q(t)$ function approaches delta function behavior with increasing M, resulting in improved per-
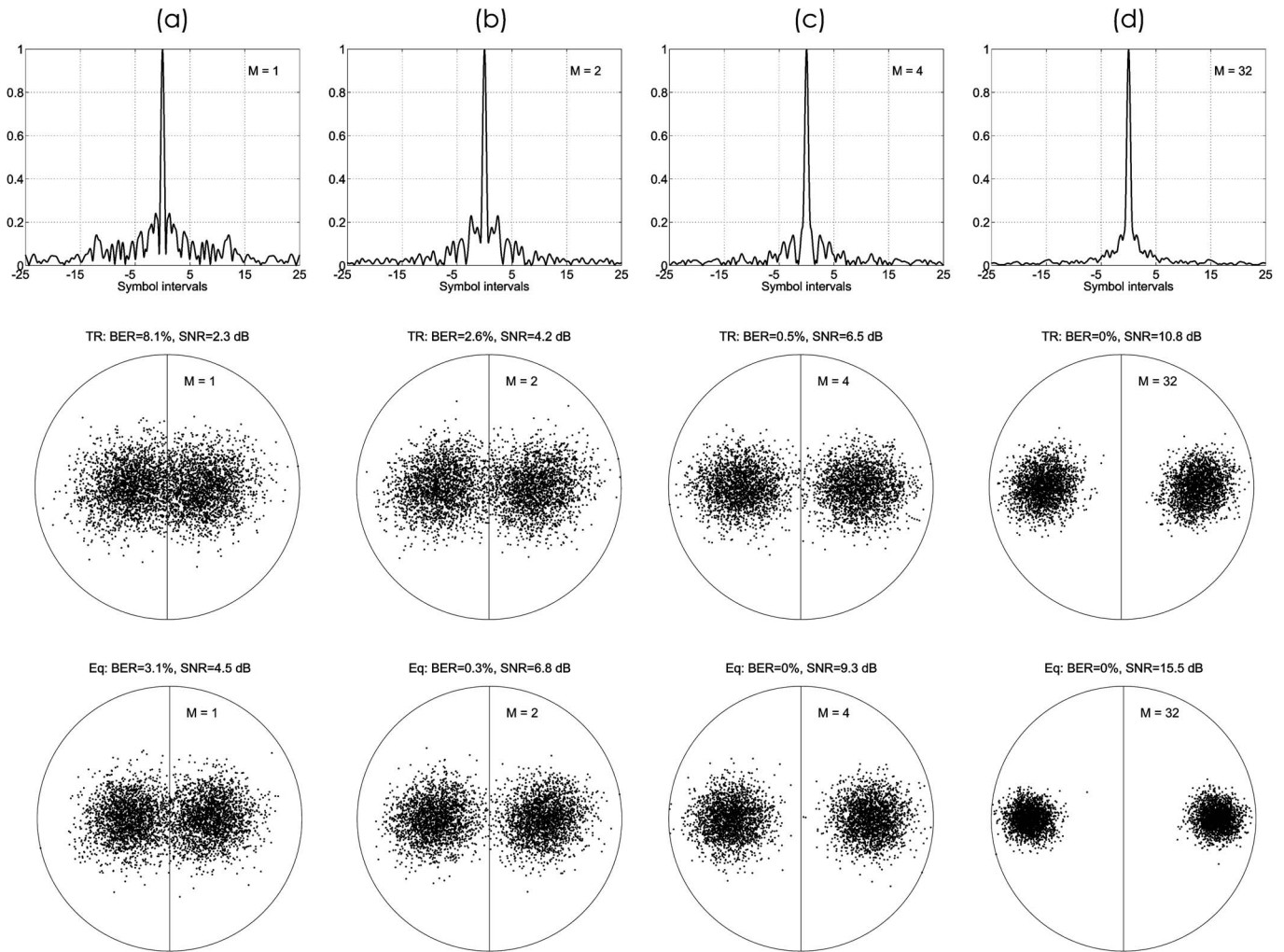
FIG. 7. Performance of multi-channel processing for various numbers of receivers M: (a) $M=1$ (single element), (b) $M=2$, (c) $M=4$, and (d) $M=32$ (entire array). The normalized $q(t)$ functions are displayed on the top row. The scatter plots are shown in the middle row for time reversal alone (Δ) and the bottom row for time reversal combined with an adaptive DFE ($\bigcirc$).

formance for time reversal communications. The middle and bottom panels are the scatter plots for time reversal alone (Δ) and time reversal combined with an adaptive DFE (o), respectively. The scatter plots suggest that as few as two receivers (or 2 m array aperture) can provide reasonable performance in this example.

V. PERFORMANCE: MOVING SOURCE

In this section, passive time reversal communications are investigated between a moving source and the VRA separated by 4.2 km as shown in Fig. 8(a). The probe source was an ITC-2007 (formerly ITC-1000) towed at about 4 knots at 70 m depth away from the VRA. The source level was 200 dB re 1 μPa. The channel probe signal was a 100 ms, 2–4 kHz LFM chirp and the corresponding channel impulse responses (envelope) are shown in Fig. 8(b) indicating a delay spread of about 100 ms. Each data symbol $g_0(t)$ was a 1 ms, 3 kHz continuous wave tone, as opposed to the chirp signal used for the fixed source in Sec. IV. The symbol rate was $R=1000$ symbols/s using BPSK modulation. The communication sequence was 9 s-long with $N=9002$ symbols and the spectral efficiency is 1 bit/s/Hz. As in the fixed

source case, the overhead resulting from a probe transmission and 100 training symbols was less than 5%. In the presence of source motion, a rough estimate of the Doppler shift is required in order to re-sample the original data.

A. Doppler estimation and resampling

Figure 9 shows the block diagram for Doppler compensation processing. First, a coarse estimate of the Doppler shift arising from source motion is obtained from the initial phase tracking applied to the original data at the carrier frequency $f_c=3$ kHz. The result for the bottom element is displayed in Fig. 10(a) where the slope corresponds to the Doppler shift of $\hat{f}_d=-4.710$ Hz. Note that no separate signaling scheme (e.g., a pilot tone[25]) is required to estimate the Doppler shift.

The next step is to re-sample the original data using a new sampling frequency of $\tilde{f}_s=f_s+\hat{f}_d$ to remove the Doppler shift. An efficient polyphase interpolator[26] and linear interpolation[27] is used for sampling rate conversion since the Doppler shift is less than 0.2%. Phase tracking applied to resample data is shown in Fig. 10(b) indicating that there is a
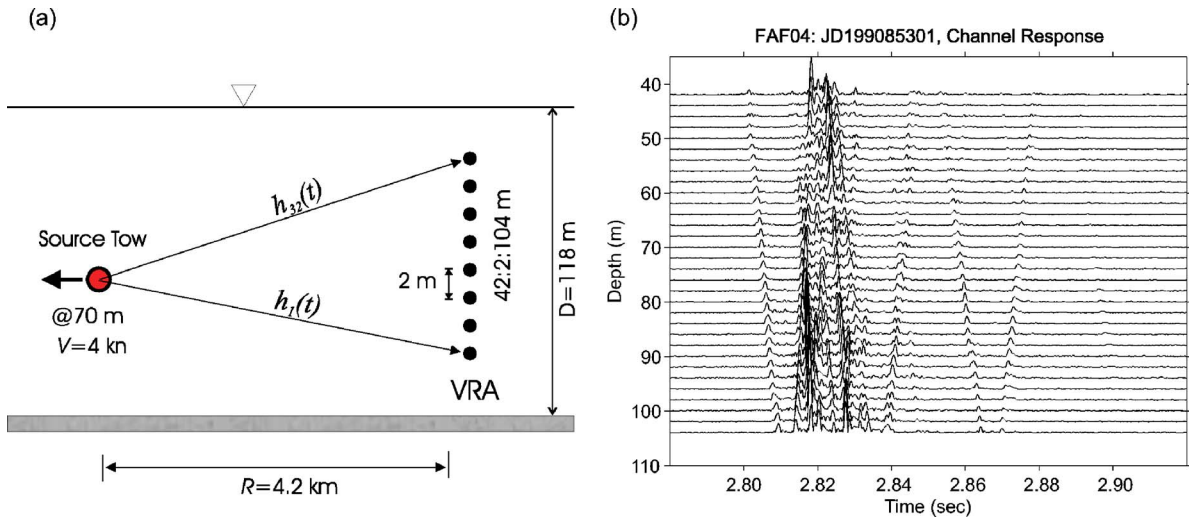
FIG. 8. (Color online) (a) Schematic of passive time reversal communications with a moving source at about 4 knots. (b) The channel responses (envelope) received by the vertical receiver array from a probe source at 70 m depth and 4.2 km range.

residual Doppler shift of $\hat{f}_d$=0.064 Hz. The overall Doppler shift is then f_d=−4.710+0.064=−4.646 Hz. There also is a small Doppler shift due to mismatch in sampling rate (f_m =−0.045 Hz) which was observed in our previous experiment.[13] The source velocity can be estimated assuming a sound speed of c=1508 m/s from Fig. 3:

$$\hat{v} = c \left[\frac{f_d - f_m}{f_c} \right] \approx -2.3 \text{ m/s}. \tag{3}$$

The ship speed during this experiment was 4.2 knots (2.1 m/s) according to the navigation data. For a single receiver case (M=1), Doppler compensation was applied independently to each element. The mean Doppler shift was −4.702 Hz with a standard deviation of 0.051 Hz. For the multi-element case (M>1), we applied the same Doppler shift estimated for the single bottom element to re-sample all receiver elements.

B. Single receiver: M=1

The performance of single element processing is illustrated in Fig. 11 in terms of BER and SNR_o using two approaches: time reversal alone (Δ) and the combination of time reversal and adaptive channel equalization (○). Note that time reversal alone (Δ) shows very poor performance such that SNR_o=−1.6–2.7 dB and BER=6%–30%, which is not surprising. Time reversal involves a correlation process (matched filtering) using the measured channel probe signal, assuming that the channel does not vary during the transmis-

sion of a data packet. However, the channel responses continue to evolve over time due to source motion even when the environmental fluctuations are minimal. Consequently, the matched filtering introduces an undesirable mismatch which gradually changes over time (9 s) even after re-sampling. This is the limitation of time reversal approach unless it is followed by an adaptive channel equalizer to compensate for the channel variations due to source motion. Therefore we focus mainly on the combined approach (○) in this subsection.

It is interesting that the performance in the middle of the water column (60–90 m) is worse with BER of 10%–30% while some receivers above and below the region show reasonable performance with BER less than 1%. Examples of scatter plots are displayed in Fig. 11(b) for two different depths: 50 m (best) and 84 m (worst). There are no bit errors at 50 and 94 m (no marker shown). Note also the symmetry between the BER (○) and SNR_o (○) which is the reciprocal of the MSE [See Eq. (2)]. In general, the output SNR_o (○) shows a similar trend as the input SNR (∗) which varies around 26–36 dB depending on the receiver depth while the input SNR displayed is offset by 20 dB for convenience. The large difference between the input and output SNRs is not well understood, but is due in part to the differential Doppler between different ray paths which leads to overall Doppler spread. In fact, a large discrepancy (10–15 dB) in the presence of strong multipath is also reported in Ref. 27 for a moving source.

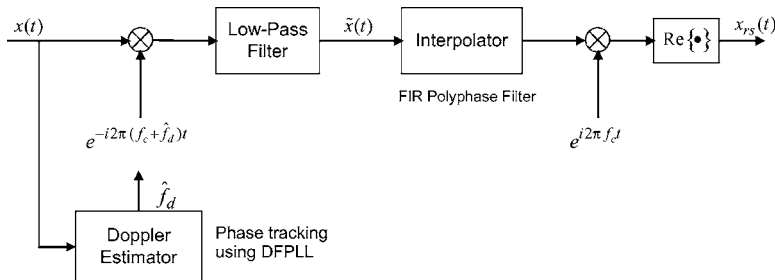Since the symbol rate is approximately equal to the sig-

FIG. 9. Block diagram for Doppler compensation processing. A Doppler shift $\hat{f}_d$ is estimated from initial phase tracking results using a DFPLL. Linear interpolation is carried out on the complex base band signal $\tilde{x}(t)$ after carrier phase correction and $x_{rs}(t)$ is the output signal re-sampled using the new sampling frequency of $\hat{f}_s=f_s+\hat{f}_d$.
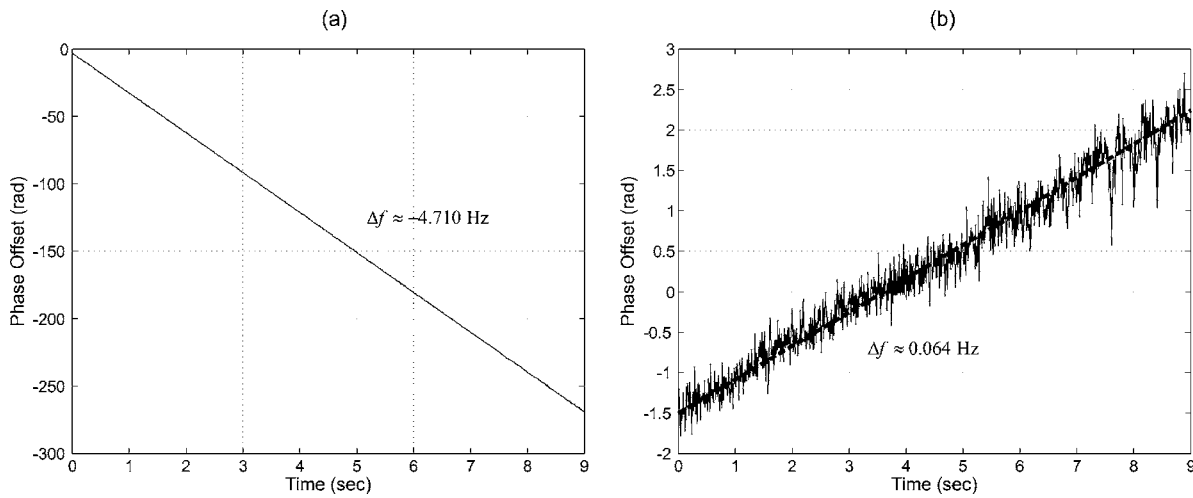
FIG. 10. Phase tracking results using a DFPLL applied to: (a) original data and (b) re-sampled data. A coarse Doppler estimate of $\hat{f}_d = -4.710$ Hz is obtained from (a). Plot (b) indicates that there is a residual Doppler shift of about $\hat{f}_d = 0.064$ Hz.

nal bandwidth[24] of 1 kHz (i.e., $W \approx 1/T$), we can use a FSE with feedforward tap spacing of $(1/2)T$ with RLS forgetting factor of 0.99. A linear equalizer has been applied to array elements in the middle of the water column and two additional depths (48 and 104 m) where the BER is greater than 10%, as mentioned in Sec. IV A, and the number of taps is $n_f = 20$. The remaining depths employ an adaptive DFE with $n_f = 20$ and $n_b = 8$.

C. Multiple receivers

The impact of spatial diversity in the presence of source motion is illustrated in Fig. 12. The performance of time reversal communications is shown in terms of (a) output SNR_o and (b) BER as a function of the number of receivers M for two different approaches: time reversal alone (Δ) and time reversal combined with an adaptive DFE ($\bigcirc$). There are no errors beyond $M = 3$ for the combination ($\bigcirc$) in Fig. 12(b). As before, the elements are selected sequentially from

the bottom. Except when $M = 1$, where a linear equalizer with $n_f = 16$ has been employed, an adaptive DFE is used with $n_f = 20$ and $n_b = 8$ and the RLS forgetting factor is 0.99.

Three observations can be made. First, the performance characteristics are very similar to those shown earlier in Fig. 6 such that the initial significant improvement is followed by a slow increase then either a minimal gradual improvement ($\bigcirc$) or saturation (Δ). On the other hand, the combination ($\bigcirc$) outperforms time reversal alone (Δ) as much as 13 dB as compared to 5 dB for the stationary source case. The saturation effect is visible in both BER and SNR_o. This observation clearly indicates that the channel variation due to source motion requires channel adaptivity and the time reversal approach should be used in conjunction with an adaptive channel equalizer to compensate for the channel variations. Finally, the input SNR ($*$) shows similar behavior to the output SNR ($\bigcirc$) while there is about 25 dB discrepancy as in Fig. 11. Note that the input SNR ($*$) displayed is offset by 20 dB.
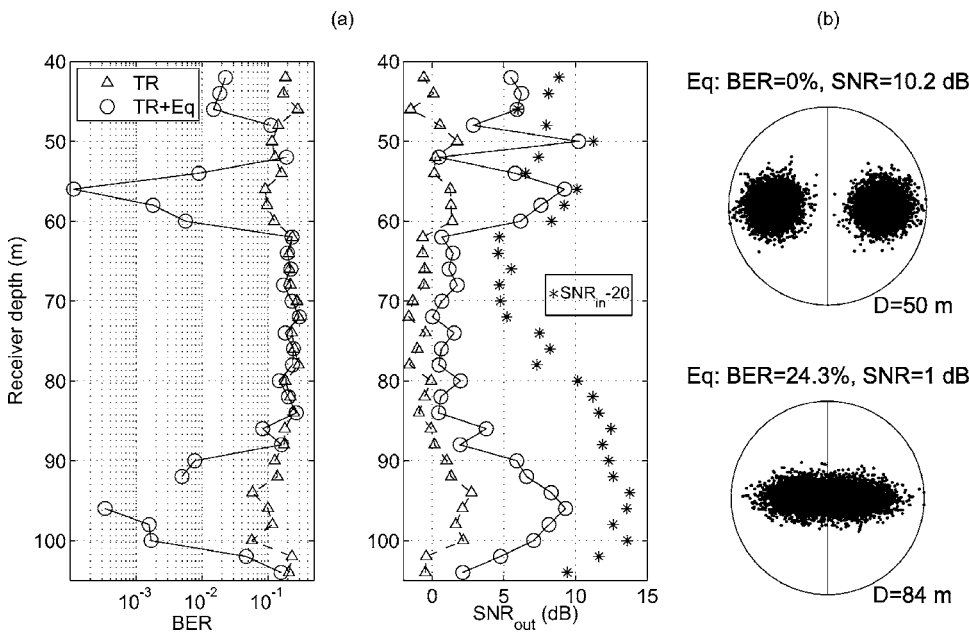

FIG. 11. Performance of single element processing: time reversal alone (Δ) and time reversal combined with an adaptive channel equalizer ($\bigcirc$). (a) BER and SNR_o as a function of receiver depth. The input SNR ($*$) is also displayed on the right column with an offset of 20 dB. (b) Example of scatter plots of time reversal combined with channel equalization for two different receiver depths: 50 and 84 m.
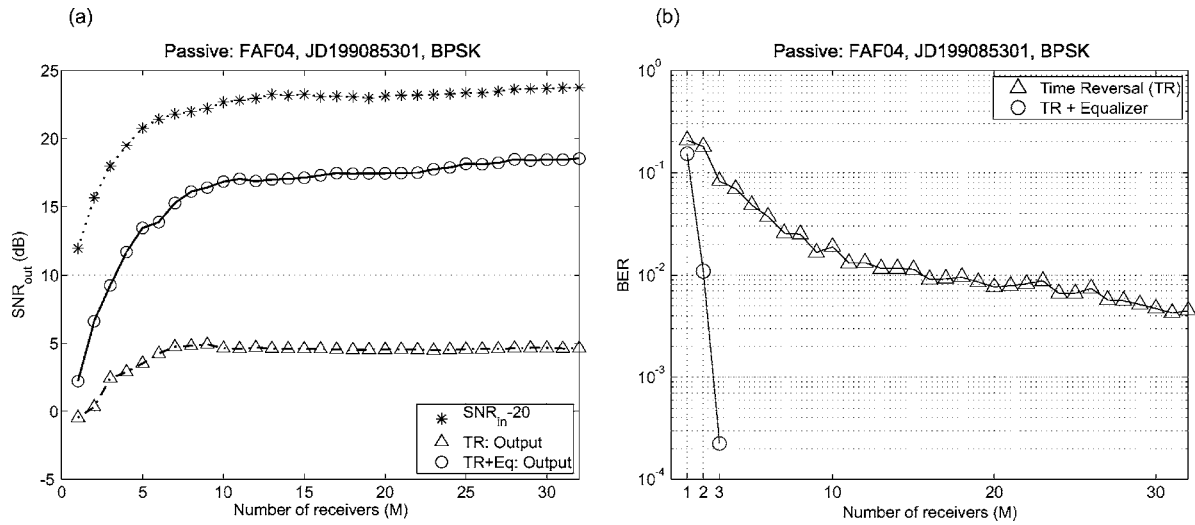
FIG. 12. Performance of multi-channel processing as a function of the number of receiver elements M: time reversal alone (Δ) and time reversal combined with an adaptive DFE ($\bigcirc$). (a) Output SNR$_o$. The input SNR ($*$) is also displayed with an offset of 20 dB. (b) BER. The combination ($\bigcirc$) shows no errors beyond $M=3$.

A few examples of scatter plots corresponding to Fig. 12 are displayed in Fig. 13 for $M=1$, 2, 3, and 10. The top panels show that the $q(t)$ function approaches a delta function with increasing M. The middle panels confirm again that
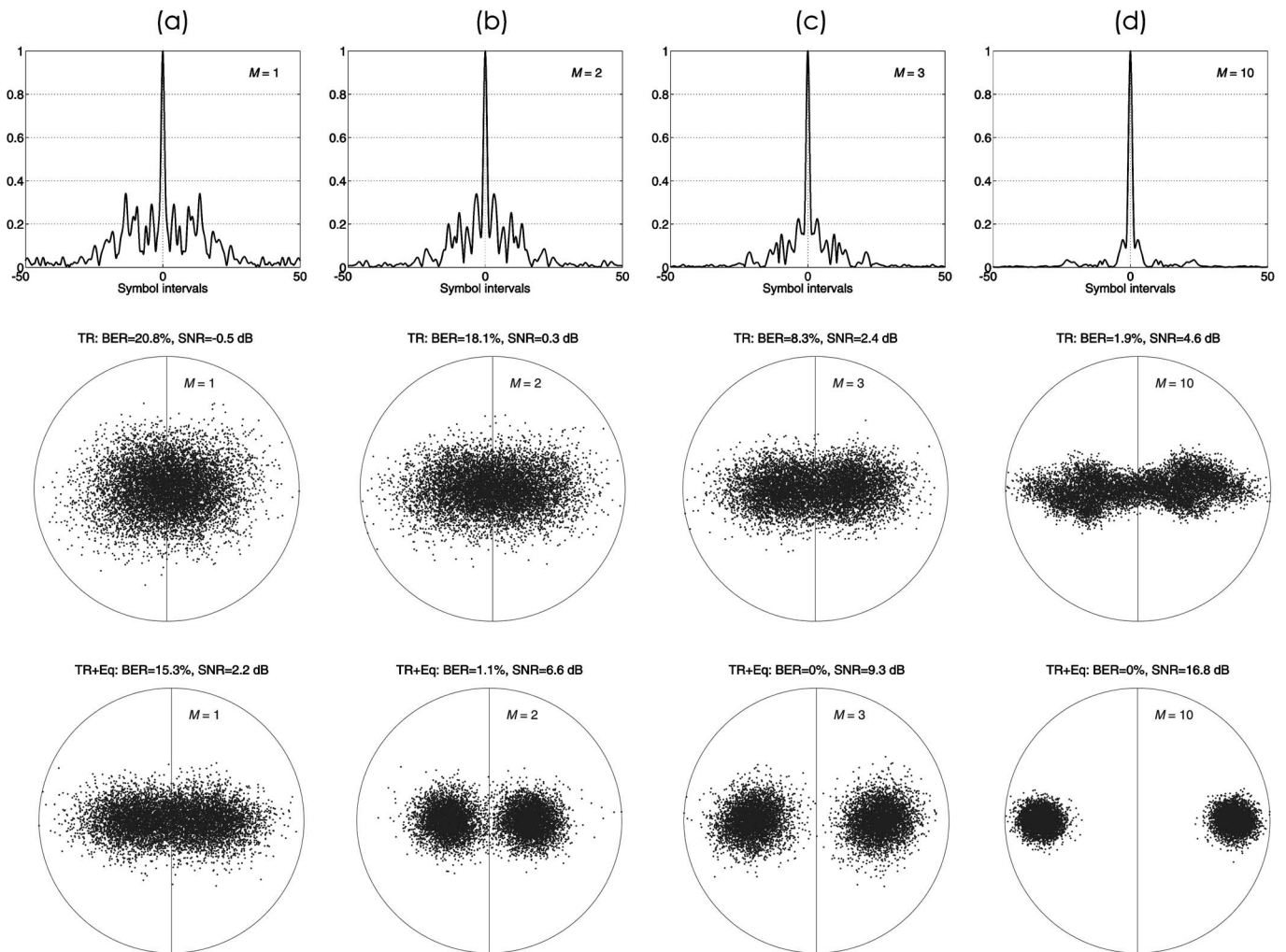

FIG. 13. Performance of multi-channel processing for various numbers of receivers M: (a) $M=1$ (single element), (b) $M=2$, (c) $M=3$, and (d) $M=10$. The normalized $q(t)$ functions are displayed on the top row. The scatter plots are shown in the middle row for time reversal alone (Δ) and the bottom row for time reversal combined with an adaptive DFE ($\bigcirc$).

the performance of time reversal alone (Δ) cannot be improved with increasing M unless the channel variations are accounted for by an adaptive channel equalizer as shown in the bottom (o). The scatter plots suggest that as few two receiver elements (or 2 m aperture) can provide reasonable performance in this example.

VI. CONCLUSION

Time reversal mirrors, either active or passive, exploit spatial diversity to achieve spatial and temporal focusing, a useful property for communications in an environment with significant multipath. Taking advantage of spatial diversity involves using a number of receivers distributed in space. While the analysis is equally applicable to the active case, for practical purposes we investigated the impact of spatial diversity in passive time reversal communications between a single probe source and a vertical receive array using the data from our July 2004 experiment. The probe source was either fixed (90 m depth and 10 km range) or moving at about 4 knots (70 m depth and 4.2 km range) from the 32-element vertical receiving array spanning the water column from 42 to 104 m with 2 m spacing in 118 m deep water, operating in the 2–4 kHz band. The performance of two different approaches was compared in terms of output signal-to-noise ratio and bit error rate as a function of the number of receivers: (1) time reversal alone and (2) time reversal combined with adaptive channel equalization.

Two conclusions have been made. First, approach (1) saturates when there is no additional gain from spatial diversity given the channel complexity. Second, approach (2) always outperforms approach (1) because the adaptive equalizer simultaneously eliminates the residual ISI and compensates for channel fluctuations if any exist. This is especially true for a moving source which introduces time-varying channel responses such that the performance enhancement amounts up to 13 dB as compared to 5 dB for a fixed source case. Finally, experimental results around 3 kHz with a 1 kHz bandwidth illustrate that as few as two or three receivers (i.e., 2 or 4 m array aperture) can provide reasonable performance at ranges of 10 km (fixed source) and 4.2 km (moving source) in 118 m deep shallow water.

ACKNOWLEDGMENT

[1]G. Edelmann, T. Akal, W. Hodgkiss, S. Kim, W. Kuperman, H. Song, and T. Akal, "An initial demonstration of underwater acoustic communication using time reversal mirror," IEEE J. Ocean. Eng. **27**, 602–609 (2002).

[2]A. Silva, S. Jesus, J. Gomes, and V. Barroso, "Underwater acoustic communications using a virtual electronic time-reversal mirror approach," *Proc. Fifth European Conference on Underwater Acoustics*, 531–536 (2000).

[3]D. Rouseff, D. Jackson, W. Fox, C. Jones, J. Ritcey, and D. Dowling, "Underwater acoustic communications by passive-phase conjugation: Theory and experimental results," IEEE J. Ocean. Eng. **26**, 821–831 (2001).

[4]G. Lerosey, J. de Rosney, A. Tourin, A. Derode, G. Montaldo, and M. Fink, "Time reversal of electromagnetic waves," Phys. Rev. Lett. **92**, 193904 (2004).

[5]H. Nguyen, J. Andersen, and G. Pederson, "The potential use of time reversal techniques in multiple element antenna systems," IEEE Commun. Lett. **9**, 40–42 (2005).

[6]B. E. Henty and D. D. Stancil, "Multipath-enabled super-resolution for rf and microwave communication using phase-conjugate arrays," Phys. Rev. Lett. **93**, 243904 (2004).

[7]W. A. Kuperman, W. S. Hodgkiss, H. C. Song, T. Akal, C. Ferla, and D. Jackson, "Phase conjugation in the ocean: Experimental demonstration of an acoustic time-reversal mirror," J. Acoust. Soc. Am. **103**, 25–40 (1998).

[8]C. Feuillade and C. Clay, "Source imaging and sidelobe suppression using time-domain techniques in a shallow-water waveguide," J. Acoust. Soc. Am. **92**, 2165–2172 (1992).

[9]M. Stojanovic, J. A. Capitovic, and J. G. Proakis, "Adaptive multi-channel combining and equalization for underwater acoustic communications," J. Acoust. Soc. Am. **94**, 1621–1631 (1993).

[10]M. Stojanovic, "Retrofocusing techniques for high rate acoustic communications," J. Acoust. Soc. Am. **117**, 1173–1185 (2005).

[11]G. Edelmann, H. Song, S. Kim, W. Hodgkiss, W. Kuperman, and T. Akal, "Underwater acoustic communication using time reversal," IEEE J. Ocean. Eng. **30**, 852–864 (2005).

[12]H. Song, W. Hodgkiss, W. Kuperman, M. Stevenson, and T. Akal, "Improvement of time reversal communications using adaptive channel equalizers," IEEE J. Ocean. Eng. [in press (2006)].

[13]H. Song, P. Roux, W. Hodgkiss, W. Kuperman, T. Akal, and M. Stevenson, "Multiple-input/multiple-output coherent time reversal communications in a shallow water acoustic channel," IEEE J. Ocean. Eng. **31**, 170–178 (2006).

[14]D. R. Dowling, "Acoustic pulse compression using passive phase-conjugate processing," J. Acoust. Soc. Am. **95**, 1450–1458 (1994).

[15]J. Flynn, J. Ritcey, D. Rouseff, and W. Fox, "Multichannel equalization by decision-directed passive phase conjugation: Experimental results," IEEE J. Ocean. Eng. **29**, 824–836 (2004).

[16]M. Stojanovic, J. A. Capitovic, and J. G. Proakis, "Reduced-complexity spatial and temporal processing of underwater acoustic communication signals," J. Acoust. Soc. Am. **98**, 961–972 (1995).

[17]Q. Wen and J. Ritcey, "Spatial diversity equalization applied to underwater communications," IEEE J. Ocean. Eng. **19**, 227–241 (1994).

[18]A. B. Baggeroer, W. A. Kuperman, and P. N. Mikhalevsky, "An overview of matched field methods in ocean acoustics," IEEE J. Ocean. Eng. **18**, 401–424 (1993).

[19]R. K. Brienzo and W. S. Hodgkiss, "Broadband matched-field processing," J. Acoust. Soc. Am. **94**, 2821–2831 (1993).

[20]T. C. Yang, "Correlation-based decision-feedback equalizer for underwater acoustic communications," IEEE J. Ocean. Eng. **30**, 865–880 (2005).

[21]T. Yang, "Temporal resolutions of time-reversed and passive-phase conjugation for underwater acoustic communications," IEEE J. Ocean. Eng. **28**, 229–245 (2003).

[22]H. C. Song and A. Dotan, "Comments on retrofocusing techniques for high rate acoustic communications [J. Acoust. Soc. Am. **117**, 1173–1185 (2005)]," submitted to J. Acoust. Soc. Am. (2006).

[23]M. Stojanovic, J. A. Capitovic, and J. G. Proakis, "Phase-coherent digital communications for underwater acoustic channels," IEEE J. Ocean. Eng. **19**, 110–111 (1994).

[24]J. Proakis, *Digital Communications* (McGraw–Hill, New York, 2001).

[25]J. Dhanoa, R. Ormondroyd, and E. Hughes, "An improved digital communication system for doubly-spread underwater acoustic channel using evolutionary algorithms," in *Proc. Oceans 2003*, 109–114 (2003).

[26]M. Johnson, L. Freitag, and M. Stojanovic, "Improved doppler tracking and correction for underwater acoustic communications," in *Proc. IC-ASSP'97*, 575–578 (1997).

[27]B. Sharif, J. Neashan, O. Hinton, and A. Adams, "A computationally efficient doppler compensation system for underwater acoustic communication," IEEE J. Ocean. Eng. **25**, 52–61 (2000).